Competition between $T = 1$ and $T = 0$ pairing in pf-shell nuclei with $N = Z$

H. Sagawa,[1,2] Y. Tanimura,[3] and K. Hagino[3]
[1]*Center for Mathematics and Physics, the University of Aizu, Aizu-Wakamatsu, 965-8580, Japan*
[2]*RIKEN Nishina Center, Wako, 351-0198, Japan*
[3]*Department of Physics, Tohoku University, Sendai 980-8578, Japan*
(Received 18 December 2012; revised manuscript received 8 February 2013; published 7 March 2013)

The pairing correlation energy for two-nucleon configurations with the spin-parity and isospin of $J^\pi = 0^+$, $T = 1$ and $J^\pi = 1^+$, $T = 0$ are calculated with $T = 1$ and $T = 0$ pairing interactions, respectively. To this end, we consider the $(1f2p)$-shell-model space, including single-particle angular momenta of $l = 3$ and $l = 1$. It is pointed out that a two-body matrix element of the spin-triplet $T = 0$ pairing is weakened substantially for the $1f$ orbits, even though the pairing strength is much larger than that for the spin-singlet $T = 1$ pairing interaction. In contrast, the spin-triplet pairing correlations overcome the spin-singlet pairing correlations for the $2p$ configuration, for which the spin-orbit splitting is smaller than that for the $1f$ configurations, if the strength for the $T = 0$ pairing is larger than that for the $T = 1$ pairing by 50% or more. Using the Hartree-Fock wave functions, it is also pointed out that the mismatch of proton and neutron radial wave functions is at most a few percent level, even if the Fermi energies are largely different in the proton and neutron mean-field potentials. These results imply that the configuration with $J^\pi = 0^+$, $T = 1$ is likely in the ground state of odd-odd pf-shell nuclei even under the influence of the strong spin-triplet $T = 0$ pairing, except at the middle of the pf shell, in which the odd proton and neutron may occupy the $2p$ orbits. These results are consistent with the observed spin-parity $J^\pi = 0^+$ for all odd-odd $N = Z$ pf-shell nuclei except for $^{58}_{29}$Cu, which has $J^\pi = 1^+$. The magnetic moment of a $(J^\pi, T) = (1^+, 0)$ state is also discussed in order to show a manifestation of the change of the shell-model scheme from jj coupling to LS coupling.

DOI: 10.1103/PhysRevC.87.034310 PACS number(s): 21.10.−k, 21.30.Fe, 21.60.−n, 27.40.+z

I. INTRODUCTION

The role of neutron-proton (n-p) isoscalar spin-triplet ($T = 0$, $S = 1$) pairing interaction in finite nuclear systems has been discussed for a long time [1–4]. It is known that the isoscalar spin-triplet pairing interaction is stronger than the isovector spin-singlet ($T = 1$, $S = 0$) pairing interaction in the nuclear matter [5,6]. Nevertheless, the nuclei are observed to favor the spin-singlet $T = 1$ pairing between identical particles. A straightforward explanation for this puzzle is that most of stable nuclei have different numbers of neutrons and protons, and thus protons and neutrons occupy different single-particle orbits near the Fermi surface, which leads to an inhibition of a $T = 0$ pair.

Even in nuclei with the equal number of protons and neutrons, the $J = 1$, $T = 0$ (n-p) pairing is not a favorable correlation compared with the $J = 0$, $T = 1$ pairing as is seen in the ground-state spins of odd-odd nuclei in the mass region above $A \geqq 20$ [2]. It has been suggested that the nuclear spin-orbit field largely suppresses the spin-triplet pairing much more than the spin-singlet pairing [7–9]. While so far no clear evidence has been found which shows the role of $T = 0$ pairing in the nuclear ground state, the manifestation of the spin-triplet pairing has been discussed in the high-spin states [10,11] and also in the Gamow-Teller giant resonances in $N = Z$ nuclei [12].

In this paper, we study the quenching of two-body matrix elements for the $T = 0$ pairing interaction in the jj coupling scheme in comparison with that for the $T = 1$ pairing interaction. Its consequence on the correlation energies is also discussed for the $J^\pi = 0^+$ and the $J^\pi = 1^+$ states in the $(1f2p)$-shell-model configurations by using Hartree-Fock (HF) single-particle wave functions. The Coulomb interaction is taken into account properly in the HF potential.

The paper is organized as follows: In Sec. II, we study the two-body matrix elements for the $T = 0$ and $T = 1$ pairing interactions. We also discuss the overlap of neutron and proton HF single-particle states for the $(1f2p)$-shell-model configurations. The competition between the energy gains for the $T = 0$ and $T = 1$ pairing interactions is studied in Sec. III by diagonalizing the pairing Hamiltonian with the $1f$ and $2p$ configurations. In Sec. IV, the magnetic moment of ($J^\pi = 1^+$, $T = 0$) state is calculated. A summary is then given in Sec. V.

II. $T = 0$ and $T = 1$ TWO-BODY PAIRING INTERACTIONS

We adopt a separable form of the pairing interaction in this paper. The spin-singlet $T = 1$ pairing interaction then reads

$$V^{(T=1)}(\mathbf{r}, \mathbf{r}') = -G^{(T=1)} \sum_{i,j} P^{(1,0)\dagger}_{i,i}(\mathbf{r}, \mathbf{r}') P^{(1,0)}_{j,j}(\mathbf{r}, \mathbf{r}'), \quad (1)$$

where the pair field operator is defined as

$$P^{(T,S)\dagger}_{i,j}(\mathbf{r}, \mathbf{r}') = \delta_{l_i,l_j} \sqrt{2l_i + 1} [a^\dagger_i a^\dagger_j]^{(T,S)} \psi_i(\mathbf{r})^* \psi_j(\mathbf{r}')^*, \quad (2)$$

with a single-particle wave function $\psi(\mathbf{r})$. Here, $a^\dagger_i$ and a_i are the creation and annihilation operators for the single-particle configuration i, respectively. The pairing strength $G^{(T=1)}$ is fit to the empirical pairing gaps [6,8,13] and is given by

$$G^{(T=1)} = \frac{24}{A}\ (\text{MeV}). \quad (3)$$

Even though the value in Eq. (3) is a reasonable choice for the one major shell-model space calculations [6,8,13], the absolute value of the pairing strength should not be taken seriously since it depends on the model space adopted. It was pointed out in Ref. [14] that the separable form of pairing interaction is quite useful as much as nonseparable realistic Hamiltonians adopted in shell-model calculations.

The spin-triplet $T = 0$ pairing is also given by a similar separable form,

$$V^{(T=0)}(\mathbf{r},\mathbf{r}') = -fG^{(T=1)} \sum_{i\geqq i',j\geqq j'} P^{(0,1)\dagger}_{i,i'}(\mathbf{r},\mathbf{r}')P^{(0,1)}_{j,j'}(\mathbf{r},\mathbf{r}'), \tag{4}$$

where the scaling factor f is varied between 1 and 2 for the strength of the $T = 0$ pairing interaction. It should be noticed that, for the $T = 0$ pairing, the pair configurations are constructed not only with the same orbit with $(l_i = l_{i'},\ j_i = j_{i'})$ but also with the spin-orbit partner orbits with $(l_i = l_{i'},\ j_i = j_{i'} \pm 1)$.

The two-body matrix element for the $T = 1$ pairing is evaluated to be

$$\langle (j_i j_i)T = 1, J = 0|V^{(T=1)}|(j_j j_j)T = 1, J = 0\rangle = -\sqrt{(j_i + 1/2)(j_j + 1/2)}\, G^{(T=1)} I^2_{ij}, \tag{5}$$

where I_{ij} is the overlap integral given by

$$I_{ij} = \int \psi_i(\mathbf{r})^* \psi_j(\mathbf{r}) d\mathbf{r}, \tag{6}$$

with the HF single-particle wave function $\psi_i(\mathbf{r})$. For the $T = 0$ pairing, the two-body matrix element involves the coefficient for the transformation from the jj coupling scheme to the LS coupling scheme and is given by

$$\langle (j_1 j_2)T = 0, J = 1|V^{(T=0)}|(j_1' j_2')T = 0, J = 1\rangle$$
$$= -\left\langle \left[\left(l_1\tfrac{1}{2}\right)^{j_1}\left(l_2\tfrac{1}{2}\right)^{j_2}\right]^{J=1}\middle|\left[(l_1 l_2)^{L=0}\left(\tfrac{1}{2}\tfrac{1}{2}\right)^{S=1}\right]^{J=1}\right\rangle\left\langle \left[\left(l_1'\tfrac{1}{2}\right)^{j_1'}\left(l_2'\tfrac{1}{2}\right)^{j_2'}\right]^{J=1}\middle|\left[(l_1' l_2')^{L=0}\left(\tfrac{1}{2}\tfrac{1}{2}\right)^{S=1}\right]^{J=1}\right\rangle$$
$$\times \frac{\sqrt{2l_1+1}\sqrt{2l_1'+1}}{\sqrt{1+\delta_{j_1,j_2}}\sqrt{1+\delta_{j_1',j_2'}}} fG^{T=1}(I_{j_1 j_1'} I_{j_2 j_2'} + I_{j_1 j_2'} I_{j_1 j_2'}), \tag{7}$$

where $\langle[(l_1\frac{1}{2})^{j_1}(l_2\frac{1}{2})^{j_2}]^{J=1}|[(l_1 l_2)^{L=0}(\frac{1}{2}\frac{1}{2})^{S=1}]^{J=1}\rangle$ is the transformation coefficient, and the overlap integral I_{ij} involves both the proton and neutron wave functions. The transformation coefficient can be evaluated with the $9j$ symbol and the explicit form is summarized in Table I. The square of the transformation coefficient is $1/6$ and $1/3$ for $j_1 = j_2$ and $j_1 = j_2 \pm 1$ configurations, respectively, in the limit of large angular momentum $l \to \infty$. These values suggest large quenching of the spin-triplet pairing correlations as well as that spin-orbit partners contribute largely to the spin-triplet pairing matrix elements. On the other hand, in the small-l limit $l \to 0$ the coefficient is unity for $j = j' = l + 1/2$, and the coefficients are zero for the other three configurations. This suggests that the spin-triplet pairing is as large as the spin-singlet pairing for the pair configuration in the $s_{1/2}$ orbit, and that it is still substantially large for the configuration in the $p_{3/2}$ orbit.

TABLE I. Transformation coefficient R between the jj coupling and the LS coupling for pair wave functions, $R = \langle[(l\frac{1}{2})^j(l\frac{1}{2})^{j'}]^{J=1}|[(ll)^{L=0}(\frac{1}{2}\frac{1}{2})^{S=1}]^{J=1}\rangle$. Ω is defined as $\Omega \equiv 3(2l+1)^2$.

j	j'	R	$l = 1$	$l = 3$
$l+1/2$	$l+1/2$	$\sqrt{\frac{(2l+2)(2l+3)}{2\Omega}}$	$\frac{1}{3}\sqrt{\frac{10}{3}}$	$\frac{2\sqrt{3}}{7}$
$l+1/2$	$l-1/2$	$-\sqrt{\frac{4l(l+1)}{\Omega}}$	$-\frac{2}{3}\sqrt{\frac{2}{3}}$	$-\frac{4}{7}$
$l-1/2$	$l-1/2$	$-\sqrt{\frac{2l(2l-1)}{2\Omega}}$	$-\frac{1}{3}\sqrt{\frac{1}{3}}$	$-\frac{\sqrt{5}}{7}$
$l-1/2$	$l+1/2$	$\sqrt{\frac{4l(l+1)}{\Omega}}$	$\frac{2}{3}\sqrt{\frac{2}{3}}$	$\frac{4}{7}$

The overlap integral I_{ij} in Eqs. (5) and (7) for the n-p pairs is estimated using HF wave functions obtained with the Skyrme interaction SLy4 [15]. The single-particle energies for ^{56}Ni are shown in Fig. 1 for both neutrons and protons. As is seen in Fig. 1, the Fermi energies in the proton and neutron mean-field potentials are largely different, by about 9 MeV. Nevertheless the proton and neutron wave functions have rather similar radial shapes and the overlap integrals I_{ij} are close to 1.0, deviating at most 3%, as shown in Table II. Thus the quenching due to the mismatch of proton and neutron wave functions in the spin-triplet pairing matrix is rather small compared with that due to the transformation coefficient from the jj to LS

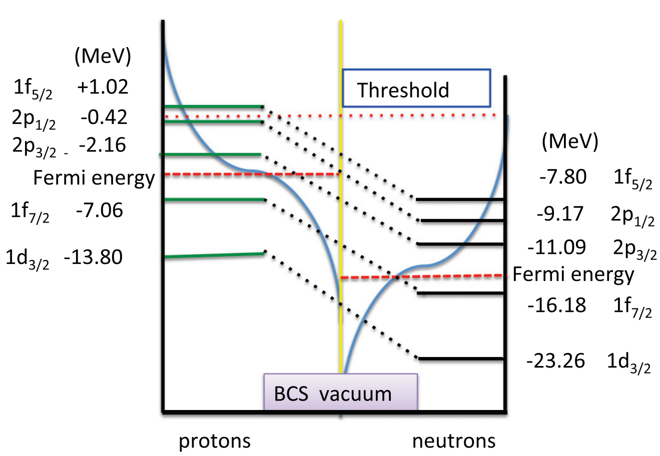

FIG. 1. (Color online) Single-particle energies of the proton and neutron orbits in ^{56}Ni, obtained with the Skyrme interaction SLy4.

TABLE II. Overlap integrals of proton and neutron Hartree-Fock wave functions, obtained with Skyrme-Hartree-Fock calculations with SLy4 interaction for ^{48}Cr, ^{56}Ni, and ^{64}Ge. The values are given in units of percent.

ν	π	^{48}Cr	^{56}Ni	^{64}Ge
$1f_{7/2}$	$1f_{7/2}$	99.9	100.	99.9
$1f_{7/2}$	$1f_{5/2}$	97.7	98.9	99.1
$1f_{5/2}$	$1f_{7/2}$	99.4	99.7	99.8
$1f_{5/2}$	$1f_{5/2}$	99.6	99.8	99.9
$2p_{3/2}$	$2p_{3/2}$	99.6	99.7	99.7
$2p_{3/2}$	$2p_{1/2}$	98.2	99.1	98.9
$2p_{1/2}$	$2p_{3/2}$	99.8	99.6	99.9
$2p_{1/2}$	$2p_{1/2}$	99.1	99.6	99.6

couplings. For this reason, we hereafter neglect the mismatch effect of the radial wave functions and the overlap integrals are taken to be unity. Notice that the overlap integrals of the pair wave functions appear also in the case of a short-range δ-type n-p pairing interaction, for which four radial wave functions are involved in the integrals.

III. PAIRING CORRELATION ENERGY FOR pf-SHELL CONFIGURATIONS

Let us next discuss the energy gain due to the pairing correlation; that is, the pairing correlation energy. Figure 2 shows the pairing gain energies for the p-orbit ($l = 1$) and the f-orbit ($l = 3$) configurations as a function of the scaling factor f for the $T = 0$ pairing. The energies for both the $J^\pi = 0^+$ state with the isospin $T = 1$ and the $J^\pi = 1^+$ state with the isospin $T = 0$ are shown in the figure. To this end, we diagonalize the pairing Hamiltonians separately for the p- and f-orbit configurations in order to disentangle the role of the pairing and the spin-orbit interactions in a transparent way. For the $l = 1$ case, the $(2p_{3/2})^2$ and $(2p_{1/2})^2$ configurations are available for the $J^\pi = 0^+$ state, while the $(2p_{3/2}2p_{1/2})$ configuration is also available for the $J^\pi = 1^+$ state. In a similar way, the $(1f_{7/2})^2$ and $(1f_{5/2})^2$ configurations participate to the $J^\pi = 0^+$ state in the $l = 3$ case, and the $(1f_{7/2}1f_{5/2})$ configuration is also involved in the $J^\pi = 1^+$ state.

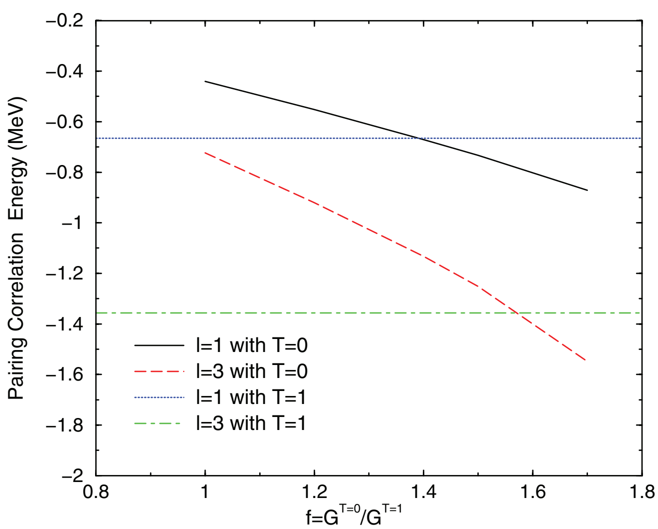

FIG. 2. (Color online) Pairing correlation energies for lowest ($J^\pi = 0^+$,$T = 1$) and ($J = 1^+$,$T = 0$) states with $l = 3$ and $l = 1$ configurations as a function of scaling factor f for $T = 0$ pairing. The strength of the spin-singlet $T = 1$ pairing interaction is fixed to be $G^{(T=1)} = 24/A$ MeV with a mass $A = 56$, while the strength for the spin-triplet $T = 0$ pairing, $G^{(T=0)}$, is varied with the factor f multiplied to $G^{(T=1)}$.

In constructing the pairing Hamiltonian, we use the spin-orbit splitting parametrized as

$$\Delta\varepsilon_{ls} = -V_{ls}(\mathbf{l} \cdot \mathbf{s}), \tag{8}$$

where the strength is taken to be [16]

$$V_{ls} = \frac{24}{A^{2/3}}\ (\text{MeV}). \tag{9}$$

This spin-orbit potential reproduces well the empirical spin-orbit splitting $\Delta\varepsilon = 7.0$ MeV between the $1f_{7/2}$ and $1f_{5/2}$ states in ^{41}Ca [17]. The uncertainly of this strength, Eq. (9), would be less than 20% in the sd- and pf-shell regions even when we adopt other empirical information on the spin-orbit splittings.

As one can see in Fig. 2, the lowest-energy state with $J^\pi = 0^+$ for the $l = 3$ case gains more binding energy than the $J^\pi = 1^+$ state for the strength factor $f < 1.5$. In the strong $T = 0$ pairing case; that is, $f \geqq 1.6$, the $J^\pi = 1^+$ state obtains more binding energy than the lowest $J^\pi = 0^+$ state. These results are largely due to the quenching of the $T = 0$ pairing matrix element by the transformation coefficient from the jj to LS coupling schemes, as we discussed in the previous section. This quenching never happens for the $T = 1$ pairing matrix element, since the mapping of the two-particle wave function between the two coupling schemes is simply implemented by a factor $\sqrt{j + 1/2}$ in Eq. (5). For the $l = 1$ case, the competition between the $J^\pi = 0^+$ and the $J^\pi = 1^+$ states is also seen in Fig. 2. Because of the smaller spin-orbit splitting in this case, the couplings among the available configurations are rather strong, and the lowest $J^\pi = 1^+$ state gains more binding energy than the $J^\pi = 0^+$ state in the case of $f \geqq 1.4$. These results are consistent with the observed spins of $N = Z$ odd-odd nuclei in the pf shell, where all the ground states have the spin-parity $J^\pi = 0^+$, except for $^{58}_{29}$Cu. The ground state of $^{58}_{29}$Cu has $J^\pi = 1^+$, since the odd proton and odd neutron occupy mainly the $2p$ orbits, where the spin-orbit splitting is expected to be much smaller than that of $1f$ orbits, as is seen in Fig. 1.

The mass-number dependence of the spin-orbit splitting is approximately determined by Eq. (9). Since the strength of the spin-orbit potential and the largest angular momentum in each major shell are proportional to $A^{-2/3}$ and $A^{1/3}$ [16], respectively, the spin-orbit splitting of the largest angular momentum states is roughly proportional to $A^{-1/3}$. On the other hand, the pairing correlation energy would be proportional to $A^{-1/2}$ as is seen in the pairing gap systematics [6,18]. Thus, the spin-orbit splitting decreases slower than the pairing correlation energy as a function of the mass number A. As a result, it is expected that the spin-orbit splitting hinders more effectively the spin-triplet pairing correlations in medium-heavy nuclei with $N = Z > 30$ compared with lighter nuclei with $N = Z < 30$. We mention that, in reality, the spin-orbit splitting decreases even more slowly than the $A^{-1/3}$ dependence; that is, 6.2 MeV for the $l = 1$ states in ^{16}O, 5.5 MeV for the $l = 2$ states in ^{40}Ca, 7.0 MeV for the $l = 3$ states in ^{56}Ni, and 7.0 MeV for the $l = 4$ states in ^{100}Sn [19,20].

It is shown that the shell-model matrix elements give the strength factor f in Eq. (4) in the range of 1.6–1.7 for both sd-shell and pf-shell configurations [9,21,22]. In Ref. [8], the ratio 1.5 is adopted to analyze the spin-triplet pairing correlations in the $N = Z$ nuclei with the shell-model calculations. These adopted values of f, together with the results shown in Fig. 2, suggest that, in the odd-odd $N = Z$ nuclei, the configuration with $J^\pi = 1^+$ is favored in the ground state rather than the $J^\pi = 0^+$ one, especially when the $p_{3/2}$ orbit is the main configuration for the valence particles. However, the implementation of spin-triplet pair condensation will not be guaranteed immediately by the spin of the ground state and may need a careful examination of many-body wave functions obtained by HF-Bogoliubov or large-scale shell-model calculations [23].

IV. MAGNETIC MOMENT

The magnetic moment may provide important information on the ground-state correlations in $N = Z$ nuclei [24]. For the isoscalar pairing correlations, the magnetic moment will show the isospin character of the ground state and also a transition of the shell-model scheme between jj and LS couplings. The magnetic moment can be evaluated by using our model wave function for a $J^\pi = 1^+$ state with $6j$ symbols:

$$\mu = \langle J, M = J, T = 0|\hat{\mu}|J, M = J, T = 0\rangle$$
$$= \sum_{(j_1,j_2),(j_1',j_2')} \frac{1}{\sqrt{6}} C_{(j_1,j_2)} C_{(j_1',j_2')} \times \left((-)^{j_1+j_2} 3 \begin{Bmatrix} j_1 & 1 & j_2 \\ 1 & j_1' & 1 \end{Bmatrix} \langle j_1||\hat{\mu}||j_1'\rangle \delta_{j_2,j_2'} + (-)^{j_1+j_2'} 3 \begin{Bmatrix} j_2 & 1 & j_1 \\ 1 & j_2' & 1 \end{Bmatrix} \langle j_2||\hat{\mu}||j_2'\rangle \delta_{j_1,j_1'} \right), \quad (10)$$

where $C_{(j_1,j_2)}$ is the amplitude of the (j_1, j_2) configuration, while $\langle j||\hat{\mu}||j'\rangle$ is the reduced matrix element for the angular momentum. The magnetic-moment operator is defined as

$$\hat{\mu} = g_s \mathbf{s} + g_l \mathbf{l}, \quad (11)$$

with $g_s^p = 5.58$, $g_s^n = -3.82$, $g_l^p = 1.0$, and $g_l^n = 0.0$ in units of nuclear magneton μ_0. For a $T = 0$ state, the isoscalar (IS) g factors $g_s^{\rm IS} = 0.88$ and $g_l^{\rm IS} = 0.5$ only give the finite contribution to the magnetic moment.

The calculated magnetic moments are shown in Fig. 3 as a function of the scaling parameter f for the $T = 0$ pairing. We adopt the p-shell configurations $(p_{3/2}, p_{1/2})$ in the calculations. The magnetic moment is gradually increasing when the $T = 0$ pairing is stronger. This is due to the fact the p-shell wave function is gradually changing from jj coupling to the LS-scheme coupling since the magnetic moment

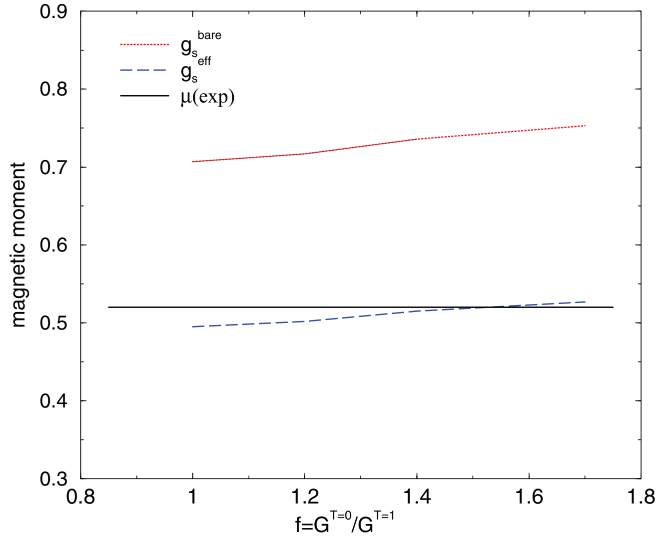

FIG. 3. (Color online) Magnetic moment μ for lowest $(J^\pi, T) = (0^+, 1)$ state with the $l = 1$ configuration as a function of scaling factor f for $T = 0$ pairing. The strength of the spin-singlet $T = 1$ pairing interaction is fixed to be $G^{(T=1)} = 24/A$ MeV with a mass $A = 56$, while the strength for the spin-triplet $T = 0$ pairing, $G^{(T=0)}$, is varied with the factor f multiplied to $G^{(T=1)}$. The spin g factor g_s is renormalized by 0.7 as the effective operator in the results shown by the dashed line, while the bare g_s factor is used in the results shown by the dotted line. The solid line denotes the experimental data of ^{58}Cu taken from Ref. [25].

is $\mu = 0.627\mu_0$ for the $(p_{3/2}p_{3/2})^{J=1,T=0}$state in the jj-coupling scheme while it becomes $0.88\mu_0$ in the $(L = 0, S = 1)^{J=1,T=0}$-coupling scheme of the p-shell configuration [24]. We also notice a quenching factor 0.7 for the spin g factor gives a good fit to the experimental value which is often used in the shell-model calculations [26]. For the IS g factor of $N = Z$ odd-odd nuclei, the large-scale shell-model calculations do not always improve the agreement with the experimental data. Especially for ^{58}Cu, a large-scale shell-model result [24] gives exactly the same g factor as that of the single-particle limit: $g = 0.63$. Thus, we need about 20% quenching of the g factor in the large-scale shell model in comparison with the empirical one g(expt.) $= 0.52$. We should also notice that the effective g factor for IS channel was pointed out to be different from the IV one [24,27]. For example, the empirical IS g factor for ^{6}Li is much larger than the Schmidt value, which never happened in the case of the IV g factor.

V. SUMMARY

We studied the spin-singlet and the spin-triplet pairing correlations in the pf-shell-model configurations for nuclei with the same proton and neutron numbers, $N = Z$. We pointed out that the spin-triplet pairing matrix element is largely quenched by the projection of the pair wave function in the jj scheme onto the $S = 1$ state. On the other hand, there is no quenching in the spin-singlet interaction since the $J^\pi = 0^+$ pair in the jj coupling scheme always has total spin $S = 0$ and the projection does not involve any quenching factor. The mismatch of the proton and neutron radial wave functions due to the large difference of the Fermi energies has also been studied by using the HF wave functions. While the difference between the proton and neutron Fermi energies is quite large, as much as 9 MeV in the $N = Z = 28$ nucleus, the overlap integral I between the proton and neutron wave functions in the spin-triplet pairing matrix have been found to be rather close to unity; the deviation being at most 3%. By diagonalizing the pairing Hamiltonian, we have shown that the spin-triplet pairing correlation energy in the $1f$-shell configuration becomes larger than the spin-singlet pairing when the strength of the spin-triplet pairing is larger than that of the spin-singlet pairing by a factor of 1.6 or more. On the other hand, for the $2p$ configuration, the spin-triplet pairing correlation becomes dominant even with the factor f of around 1.4. We studied the magnetic moment of a $(J^\pi, T) = (1^+, 0)$ state with a $2p$ configuration. The calculated value increases when the $T = 0$ pairing increases according to the change of the shell-model scheme from jj coupling to LS coupling. In this paper, we studied one n-p pair in the pf-shell configuration. It was pointed out recently that the maximum spin-aligned configuration plays an important role in many n-p pair configurations and competes with the minimum spin-aligned configuration [28]. It is an interesting future problem to study the competition between the minimum and the maximum aligned configurations in the ground and excited states in $N \sim Z$ nuclei.

ACKNOWLEDGMENTS

This work was supported through a grant-in-aid by the JSPS under the program number 24·3429 and the Japanese Ministry of Education, Culture, Sports, Science and Technology by a Grant-in-Aid for Scientific Research under program number (C) 22540262. The work of Y.T. was also supported by the Japan Society for the Promotion of Science for Young Scientists.

[1] A. L. Goodman, Nucl. Phys. A **186**, 475 (1972); Phys. Rev. C **60**, 014311 (1999).
[2] A. O. Macchiavelli *et al.*, Phys. Rev. C **61**, 041303(R) (2000); Phys. Lett. B **480**, 1 (2000).
[3] A. F. Lisetskiy *et al.*, Phys. Rev. C **68**, 034316 (2003).
[4] B. Cederwall *et al.*, Nature (London) **469**, 68 (2011).
[5] M. Baldo, U. Lombardo, and P. Schuck, Phys. Rev. C **52**, 975 (1995); L. G. Cao, U. Lombardo, and P. Schuck, *ibid.* **74**, 064301 (2006).
[6] D. M. Brink and R. Broglia, in *Cambridge Monographs on Particle Physics, Nuclear Physics and Cosmology*, Vol. 24 (Cambridge University Press, Cambridge, 2005).
[7] G. F. Bertsch, *50 Years of Nuclear BCS*, edited by R. Broglia and V. Zelevinsky (World Scientific, Singapore, 2012).
[8] A. Poves and G. Martinez-Pinedo, Phys. Lett. B **430**, 203 (1998).
[9] G. F. Bertsch and Y. Luo, Phys. Rev. C **81**, 064320 (2010).
[10] W. Satuła and R. Wyss, Phys. Lett. B **393**, 1 (1997); J. Terasaki, R. Wyss, and P. H. Heenen, *ibid.* **437**, 1 (1998).
[11] A. L. Goodman, Phys. Rev. C **63**, 044325 (2001).
[12] C. L. Bai, H. Sagawa, M. Sasano, T. Uesaka, K. Hagino, H. Q. Zhang, X. Z. Zhang, and F. R. Xu, Phys. Lett. B **719**, 116 (2013).
[13] A. Bohr and B. R. Mottelson, *Nuclear Structure*, Vol. 2 (W. A. Benjamin, Inc., Massachusetts, 1975).
[14] E. Mayo de Guerra, A. A. Raduta, L. Zamick, and P. Sarriguren, Nucl. Phys. A **727**, 3 (2003).
[15] E. Chabanat, P. Bonche, P. Haensel, J. Meyer, and R. Schaeffer, Nucl. Phys. A **627**, 710 (1997); **635**, 231 (1998); **643**, 441 (1998).
[16] A. Bohr and B. R. Mottelson, *Nuclear Structure*, Vol. 1 (W. A. Benjamin, Inc., New York, 1969), p. 218.
[17] Y. Uozumi *et al.*, Phys. Rev. C **50** 263 (1994).
[18] A. Bohr and B. R. Mottelson, *Nuclear Structure*, Vol. 1 (W. A. Benjamin, Inc., New York, 1969), p. 169.
[19] A. Bohr and B. R. Mottelson, *Nuclear Structure*, Vol. 1 (W. A. Benjamin, Inc., New York, 1969), p. 322.
[20] X. Roca-Maza, G. Colò, and H. Sagawa, Phys. Rev. C **86**, 031306(R) (2012).
[21] B. A. Brown and W. A. Richter, Phys. Rev. C **74**, 034315 (2006).
[22] M. Honma, T. Otsuka, B. A. Brown, and T. Mizusaki, Phys. Rev. C **69**, 034335 (2004); Eur. Phys. J. A **25**, 499 (2005).
[23] A. Gezerlis, G. F. Bertsch, and Y. L. Luo, Phys. Rev. Lett. **106**, 252502 (2011).
[24] S. Yeager, S. J. Q. Robinson, L. Zamick, and Y. Y. Sharon, Europhys. Lett. **88**, 52001 (2009).
[25] N. J. Stone *et al.*, Phys. Rev. C **77**, 067302 (2008).
[26] P. J. Brussard and P. W. M. Glaudmans, *Shell Model Applications in Nuclear Spectroscopy* (North-Holland, Amsterdam, 1977).
[27] L. Zamick, Phys. Rev. C **15**, 824 (1977).
[28] C. Qi, J. Blomqvist, T. Bäck, B. Cederwall, A. Johnson, R. J. Liotta, and R. Wyss, Phys. Scr. **150**, 014031 (2012).